

## FLOW BEHAVIOR OF BASAL ICE AS RELATED TO MODELING CONSIDERATIONS

by

Hitoshi Shoji and Chester C. Langway Jr.

(Ice Core Laboratory, Department of Geological Sciences, State University of New York at Buffalo, 4240 Ridge Lea Road, Amherst, New York 14226, U.S.A.)

### ABSTRACT

Simple shear tests on the bottom 17 m of basal ice from Camp Century, Greenland, were carried out in order to study the flow behavior near the bottom of an ice sheet and its implications for ice-sheet modeling. The ice core was recovered in 1966. Our experimental results show that the basal ice tested, (which contained alternating bands of dirty and clean ice) has the highest strain-rate ever reported for polycrystalline ice under simple shear. The enhancement factors obtained are interpreted in terms of fabric, ageing, and impurity. Horizontal velocity profiles are calculated using data reported previously for Camp Century and Dye 3 stations. Various depth-age relationships are compared with these data. The higher than expected shear strain-rates measured on samples of near-bottom ice from Camp Century may very well exist at other locations. If such high shear strain-rates are more prevalent than presently thought, they could have an important bearing on ages calculated by physical or mathematical models of ice sheets.

### 1. INTRODUCTION

Mechanical tests on basal ice samples from the Camp Century (77°10'N, 61°08'W) ice core, recovered in 1966, were carried out in order to study the flow behavior near the bottom of the ice sheet as related to ice-flow modeling. The relationship between strain-rate and stress with laboratory-prepared randomly oriented polycrystalline ice is well described by Glen's law (Glen 1955, Barnes and others 1971). For natural glacier ice three additional factors should be considered which enhance strain-rate: (1) fabrics (Lile 1978, Russell-Head and Budd 1979), (2) impurities (Jones and Glen 1969, Nakamura and Jones 1973), and (3) debris particles (Hooke and others 1972).

In 1966 a continuous ice core was recovered at Camp Century from the ice-sheet surface to the bottom at a depth of 1 387 m (Hansen and Langway 1966). Physical and chemical properties were analysed by Herron [S L] and Langway (1979, 1982) and Herron [M M] and Langway (1982) respectively. The bottom 17 m of this vertical ice core contains a debris-laden zone. At Camp Century the surface velocity was measured to be  $3.3 \text{ m a}^{-1}$  with a surface slope of  $3.5 \times 10^{-3} \text{ rad}$  (Mock 1968). The temperature in the bore hole varied from  $-24^\circ\text{C}$  at the surface to  $-13^\circ\text{C}$  at the bottom, with a minimum value of  $-24.7^\circ\text{C}$  at about 200 m depth (B L Hansen private communication).

A depth-age relationship (time scale 1) was calculated for Camp Century by Dansgaard and Johnsen

(1969) and by Hammer and others (1978) based on the  $\delta^{18}\text{O}$  (Dansgaard and others 1969) and microparticle (Hammer 1977[a], [b]) profiles. These data yielded an accumulation rate of  $0.382 \text{ m a}^{-1}$  at the surface, and a vertical strain-rate that has a constant value of  $3.32 \times 10^{-4} \text{ a}^{-1}$  from the surface to a distance of 429 m from the bottom, and then decreases linearly to the bottom.

Dansgaard and others (1982) compared the published Camp Century  $\delta^{18}\text{O}$  profile (Dansgaard and others 1969) with the published Dye 3  $\delta^{18}\text{O}$  profile (Dansgaard and Reeh 1982) and the deep-sea foraminifera record (Hays and others 1976), and obtained another time scale (time scale 2) for the Camp Century ice core. Time scale 2 gives much older ages for the bottom 250 m than time scale 1.

### 2. EXPERIMENTAL PROCEDURE

#### 2(a). Specimen preparation

Three samples were selected from the Camp Century basal ice core for these tests, a "dark" sample (type 1 from 1 375 m depth), an "intermediate" (or "medium") sample (type 2 from 1 377 m) and a "clear" sample (type 3 from 1 379 m). The sample classification is based on visual observations of transmitted white light through the ice core using a light table (Herron [S L] and Langway 1979). Each sample was more than 30 cm long and was cut into several specimens for microscopic observations (M) and simple shear tests (S). Samples were rough-cut with a bandsaw and the surface finished with a microtome to about  $1 \times 3 \times 10 \text{ cm}$  (for M) and  $(21.4 \pm 0.05) \times (22.4 \pm 0.2) \times (31.4 \pm 0.4) \text{ mm}$  (for S). Vertical and horizontal specimens (M) were prepared for observations of microstructure. Specimens for simple shear tests (S) were prepared so as to have the applied shear stress plane parallel to the horizontal plane of each ice-core sample. An additional specimen of type 2 was prepared so that the applied shear stress plane was inclined  $45^\circ$  from the horizontal plane so that the fabric enhancement factor could be examined.

#### 2(b). Optical microscopic observation

Grain size was measured by the intercept method (Herron [S L] and others 1982) under an optical microscope. Internal microstructure was observed and photographed for gas, liquid and solid inclusions. Evaporation pits were formed on the specimen surface by the formvar method (Higuchi 1958, Matsuda 1979) to determine the crystal orientations.

#### 2(c). Simple shear tests

The simple shear creep testing apparatus was

specially designed and constructed for this study. It was also used for the mechanical tests made on the fresh ice-core samples from the Dye 3 ice core very soon after recovery (Shoji and Langway 1982[b]). The two side faces of the specimen were frozen onto brass plates so as to have a thickness of 31.4 mm. One of the plates was fixed to the frame of the apparatus whilst the other was allowed to slide vertically with a linear motion using vertical rods driven by a controlled weight. The vertical displacement of the sliding plate was recorded with a linear voltage differential transformer (LVDT) detector. The apparatus was contained in a temperature-controlled insulated box in a laboratory cold room kept at  $-15^{\circ}\text{C}$ . Temperature was measured with copper-constantan thermocouples and maintained at  $-13^{\circ}\text{C}$  to conform with the measured value at the bottom of the Camp Century bore hole. The temperature fluctuation was within  $0.2^{\circ}\text{C}$  for each test run.

3. EXPERIMENTAL RESULTS AND DISCUSSIONS

3(a). Optical microscope observations

The general characteristics of the types of basal ice relevant to the present study are given in Table I (Herron [S L] and Langway 1979). Descriptions of the three samples tested are given in Table II.

Changes in physical properties of an ice core with time after core recovery were earlier reported using the pressure change with time of an air-bubble

(Langway 1958). This is essentially an ice deformation process centered around air bubbles and driven by a hydrostatic pressure difference between the gas in the air bubble and the ambient pressure (Shoji and Langway 1983). The internal surfaces of air bubbles in basal ice samples (types 1, 2 and 3) were observed to be very smooth compared with those of bubbles in fresh ice core (Shoji and Langway 1982[a]). This suggests that the air pressure in the gas bubbles may already be very close to ambient pressure and that the ice deformation around the air bubbles is no longer active. With the type 1 sample (dark ice), a significant decrease in color intensity was observed near the edges of the ice core. This is probably related to a process of diffusion from the center of the included impurities in the core outwards. Grain-size distribution from the center of the cross-section of the core to the periphery also revealed a large increase in grain size from 0.5 mm at the center to 3 to 4 mm near the periphery. This change in grain size is observed in specimens from both horizontal and vertical sections (Fig.1). The triple junctions of grain boundaries are mostly decorated with small-sized debris particles as shown in Figure 2(a), which clearly identify the location of grain boundaries in three dimensions. Within large ice grains near the outer core surface, chain networks of air bubbles were often observed with a comparable network size (0.5 mm) to grain size near the center of the core (Fig.2(b)). Because of

TABLE I. GENERAL CHARACTERISTICS OF BASAL ICE (CAMP CENTURY)

Color appearance	Debris concentration	Total gas content	Density at $-13^{\circ}\text{C}$	Percentage of ice type in 17 m of basal ice
	wt %	$\text{m}^3 \text{kg}^{-1}(\text{STP})$	$\text{kg m}^{-3}$	%
Clear	0.02	$(5.3 \pm 1.1) \times 10^{-5}$	$914 \pm 1$	10
Light	0.15	$(5.3 \pm 1.1) \times 10^{-5}$	$914 \pm 1$	35
Medium	0.31	$(5.3 \pm 1.1) \times 10^{-5}$	$914 \pm 1$	53
Dark	0.70	$(5.3 \pm 1.1) \times 10^{-5}$	$914 \pm 1$	2
Clear ice (overlying basal ice)	0.00	$9.5 \times 10^{-5}$	$913 \pm 1$	-

TABLE II. MICROSTRUCTURE OF BASAL ICE SAMPLES (CAMP CENTURY)

Sample no.	Color appearance	Depth from the surface (m)	Distance from the bottom (m)	Major inclusions	Minor inclusions	First quartile Degrees from vertical direction
1	Dark	1 375	12	Air bubbles, debris particles	Liquid veins, lenses	$20 \pm 3$
2	Medium	1 377	10	Air bubbles	Gas hydrates, debris particles	$10 \pm 3$
3	Clear to light	1 379	8	Air bubbles	Gas hydrates, debris particles	$10 \pm 3$

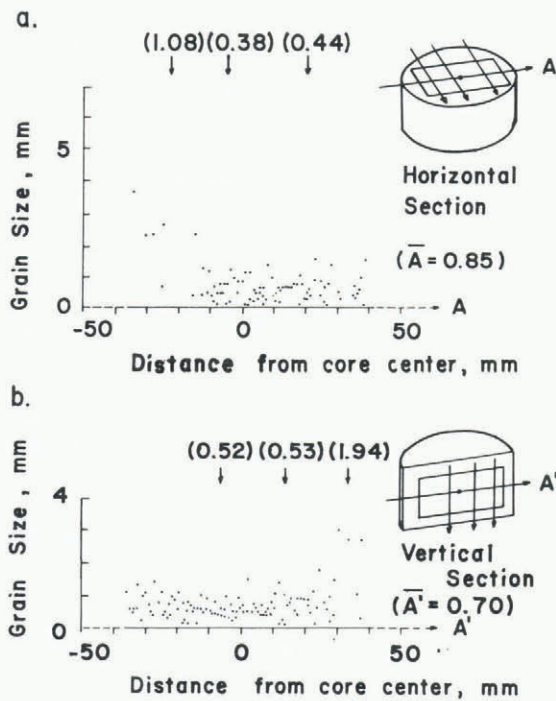


Fig.1. Grain-size distribution of type 1 sample, dark ice, with distance from ice core center. (a) horizontal section, (b) vertical section. Numerical values in parentheses are average grain sizes in mm.

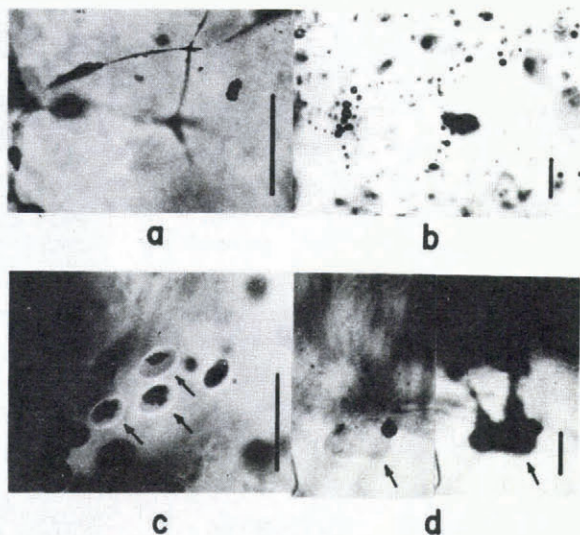


Fig.2. Microstructure of basal ice. Each vertical bar equals 0.2 mm. (a) triple junction of grain boundaries decorated with small debris particles, (b) air-bubble chain network observed within a large grain near the core surface, (c) liquid lenses (denoted by arrows) in a dark sample, (d) a transformation of a gas hydrate inclusion (left) into gas bubbles (right) under heat treatment. Arrows denote the same position at different times.

these alterations, specimens used for the shear tests were prepared from the non-recrystallized central part of the original ice core. Microscopic observations also revealed that liquid veins and lenses formed at the triple junctions of grain boundaries and grain boundary planes, respectively (Fig.2(c)). The size of the liquid inclusions increased when the temperature of the sample was increased. Oguro (1975)

showed in his studies of the growth of single ice crystals using dilute aqueous solutions that pockets of solutions were formed when the concentration of impurity ( $\text{NH}_4\text{F}$  or  $\text{NaCl}$  in his studies) in the original solution exceeded 1 000 ppm. These liquid inclusions observed in type 1 samples (dark ice) were generally accompanied by debris particles or aggregates of particles in suspension.

In the other two samples tested (clear ice, type 3, and medium ice, type 2) a very small number of gas hydrate inclusions were observed which were similar to those found in the fresh ice core from Dye 3 (Shoji and Langway 1982[a]). By using a heat treatment whereby the specimen is gradually melted under a microscope, the transformation of the gas hydrates into a large volume of individual gas bubbles, as shown in Figure 2(d), was observed. According to a phase diagram constructed by Miller (1969), an air hydrate inclusion in clathrate structure I is not stable under long-term ice-core storage (at about  $-30^\circ\text{C}$ ) and atmospheric pressure. This agrees with our observations that only a small number of gas hydrate inclusions remain for long after core recovery.

Results of ice-fabric analysis using the evaporation pit method are given in Table II (first quartile of c-axis verticality).

3(b). Simple shear tests

Each specimen was deformed more than 1.2% in shear-strain in order to obtain the necessary minimum creep rate (Russell-Head and Budd 1979). The results show that these ice specimens have the highest shear strain-rate ever reported for polycrystalline ice under simple shear (Fig.3). Specimens of types

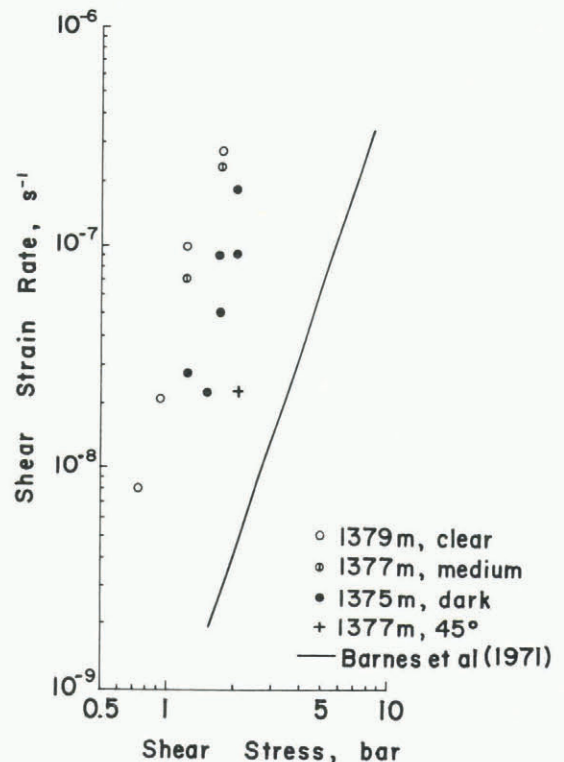


Fig.3. Logarithmic plot of shear strain-rate versus shear stress. Simple shear stress was applied along the horizontal plane of the core. Sample "1377m, 45°" was tested with the applied simple shear stress inclined at 45° from the vertical axis of the core. Experimental results on randomly oriented artificial polycrystalline ice by Barnes and others (1971) have been converted from uniaxial stress/strain-rate to shear stress/strain-rate using Nye's (1957) formula. All data points were experimentally obtained at a temperature of  $-13^\circ\text{C}$ .

TABLE III. ESTIMATION OF ENHANCEMENT FACTOR

Core site	(Date drilled) Period between recovery and testing (years)	Depth (m)	Measured enhancement factor	Estimated fabric factor	Estimated ageing factor	Remnant (impurity) factor	Remarks	Reference
Simple shear, parallel to horizontal plane (easy glide)								
Camp Century (77°10'N 61°08'W)	(1966) 13-17	1 377-1 379	40-100	4	4	3-6	Basal ice clear to medium	Present work
		1 375	20-50	2	4	3-6	Basal, dark	Present work
Dye 3 (64°12'N 43°47'W)	(1980/81) ≤0.1	235-1 293	0.5-2	0.5-2	1	1	Holocene	Shoji and Langway (1982[b])
		1 814	24	4	1	6	Wisconsin	Shoji and Langway (1982[b])
Cape Folger (66°S 111°E)	(1969) ≤3	200	2.78	2.79	1	1	Holocene	Lile (1978)
	(1974) ≤3	55-260	1.3-4	1-4	1	1	Holocene	Russell- Head and Budd (1979)
Simple shear, 45° inclined (hard glide)								
Cape Folger	(1969) ≤3	200	0.22	0.21	1	1	Holocene	Lile (1978)
Camp Century	(1966) 13-17	1 377	5	0.2	4	6	Basal, medium	Present work
Uniaxial, 45° inclined to vertical direction (easy glide)								
Byrd station (80°01'S 19°31'W)	(1968/69) 4-8	1 300	25-40	4	4	2-3	Wisconsin, (tension)	Shoji (un- published)
Dye 3	≤0.1	235-1 293	0.5-2	0.5-2	1	1	Holocene, (compression)	Shoji and Langway (1982[b])
		1 814	8-10	4	1	2-3	Wisconsin, (compression)	Shoji and Langway (1982[b])
		2 021	10	4	1	3	16 m above the bottom, (compression)	Shoji and Langway (unpublished)
Mizuho station (70°42'S 44°20'E)	(1975) 2	100	1.2	1-2	1	1	Holocene, (compression)	Shoji (1978)
Uniaxial, parallel to vertical direction (hard glide)								
Byrd station	(1968/69) 4-8	300	6	1-1.5	4	1	Holocene, (tension)	Shoji (unpublished)
		1300	1-2	0.1	4	3-5	Wisconsin, (tension)	
Dome summit (67°S 113°E)	(1969)	318	1.41	1.47	1	1	Holocene, (compression)	Lile (1978)
Dome C (74°39'S 124°10'E)	(1977/78) ≤3	?	0.25	0.1	1	3	? (compression)	Duval and Le Gac (1982)
Dye 3	≤2	1 815	0.1-0.15	0.1	1	1-2	Wisconsin, (compression)	Shoji and Langway (un- published)

TABLE III. ESTIMATION OF ENHANCEMENT FACTOR (cont.)

Torsion, around vertical direction (easy glide)								
Dome C	(1977/78) ≤3	155	1.5	1-2	1	1	Holocene	Duval and Le Gac (1982)
		?	12.5	4	1	3	?	Duval and Le Gac (1982)
Uniaxial compression, 45° inclined under hydrostatic pressure (easy glide)								
Byrd station	(1968/69) 13	1 400	8	4	1	2	Wisconsin	Azuma (un- published report)
Dye 3	(1980/81) ≤2	796	0.5-0.8	0.5-1	1	1	Holocene	Azuma and Higashi (unpublish- ed report)
		1 800+1 900	4-8	4	1	1-2	Wisconsin	Azuma and Higashi (unpublish- ed report)
		2 000	8-10	4	1	2-3	37 m above the bottom	Azuma and Higashi (unpublish- ed report)

3 and 2 (clear and medium ices) have almost equal strain-rates, which are 40 to 100 times greater than those of laboratory prepared ice, and the type 1 specimens (dark ice) have about half the strain-rate of the other two types at the same stress level. We obtained a fabric enhancement factor of two for type 1 ice and four for type 2 and 3 ice using the diagram of Russell-Head and Budd (1979). The strain-rate differences for the different types at the same stress level agrees quite well with those expected from the above fabric-factor diagram.

To investigate the hard-glide stress condition we tested another type 2 specimen with the stress direction 45° from the horizontal plane. This test resulted in a strain-rate one order of magnitude lower than that obtained by the previous easy glide orientation (Fig.3). This result also agreed with the change of fabric enhancement factor both calculated and measured by Lile (1978). Since the concentration of debris particles is less than 0.7% by weight in every sample tested (Table I), the dispersion-hardening effect of particles should be small or negligible as indicated by the experiments of Hooke and others (1972). X-ray studies show that microstructures of both impurity-doped crystals (Oguro 1975) and relaxed ice-core samples (Shoji and Higashi 1978) have either mosaic patterns or sub-boundaries. Muguruma (1969) showed that the yield-stress of single ice-crystal specimens having sub-boundaries was as low as one quarter of those not having sub-boundaries. This softening is caused by the increase in mobile dislocation density. The softening effect created by HF doping is discussed in terms of dislocation mobility by Jones and Glen (1969).

The values of enhancement factors obtained in this work and other published data enable us to calculate horizontal velocity profiles and subsequently to discuss depth-age relationships.

#### 4. APPLICATIONS TO GLACIER FLOW AND DISCUSSIONS 4(a). Strain-rate enhancement factor

Fabric enhancement factors vary from one (random plot) to four (strong single maximum plot) depending upon preferred stress direction as related to basal glide direction (Lile 1978, Russell-Head and Budd 1979). In the case of hard glide deformation with a single fabric maximum, we estimate a fabric enhancement factor value of 0.1 based on our experimental data (Table III). For a highly relaxed ice core (considerable time after core recovery), we assigned a value of four to the ageing factor, based on experiments performed on fresh and relaxed ice cores (Shoji and Langway 1982[b], Shoji unpublished) and experiments made under confined and unconfined stress conditions (Azuma unpublished). For example, experimental results of the specimens taken from a depth of 300 m 4 to 8 a after core recovery from Byrd station showed a measured enhancement factor of six in uniaxial tension tests, although the estimated fabric enhancement factor is between 1 and 1.5 (Table III). This "softening" is taken into consideration as an ageing factor resulting from the mosaic/sub-boundary structure formed during the volume relaxation process after core recovery.

Table III gives a summary of unpublished experimental strain-rate data, together with measured total enhancement factors and estimated fabric/ageing enhancement factors. The remnant factor was defined as measured enhancement factor divided by product of fabric factor and ageing factor. A remnant factor greater than one is closely related to Wisconsin ice or basal silty ice, as is shown in Table III. Experiments showed that certain types of impurities such as HF and HCl soften ice by increasing the mobility of a dislocation and/or by increasing the density of mobile dislocations (Jones and Glen 1969, Nakamura and Jones 1973). Chemical analyses made on polar ice cores reveal high Cl<sup>-</sup> contents in Wisconsin ice (Petit and

others 1981 Herron [M M] and Langway 1982). Our results also show that basal silty ice at Camp Century includes a high content of soluble impurities, although the HF content of ice cores has not been measured and the effect of other impurities such as  $SO_4^{2-}$  on the mechanical properties of ice is unknown. In this study we use the  $Cl^-$  content as an impurity factor indicator, although the measured concentration levels of  $Cl^-$  seems to be too low to have a significant effect on the strain-rate enhancement. The  $Cl^-$  concentration in both Camp Century and Dye 3 ice cores increases with distance from the bottom, and is extremely high in ice of the late-Wisconsin period (Herron [M M] and Langway 1982). The highest  $Cl^-$  level is found at locations at, or just beneath, the Holocene/Wisconsin transition, located at 232 and 251 m from the bottom at Camp Century and Dye 3, respectively. We assume an impurity enhancement factor of three for ice in which the  $Cl^-$  concentration is greater than half of that in late-Wisconsin ice. The impurity enhancement factor elsewhere is unity, except for silty ice at Camp Century which has an impurity factor of three.

4(b). Horizontal velocity profile

The estimated enhancement factors as a function of depth-interval for the Camp Century and Dye 3 ice cores are given in Table IV. Strain-rates for these

TABLE IV. ESTIMATED ENHANCEMENT FACTORS FOR CALCULATING A VELOCITY PROFILE

Camp Century

Depth interval (m)	Fabric factor	Impurity factor	Total* factor
0 - 500	1	1	1
500 - 900	2	1	2
900 - 1 155	3	1	3
1 155 - 1 267	4	3	12
1 267 - 1 370	3	1	3
1 370 - 1 387	4	3	12

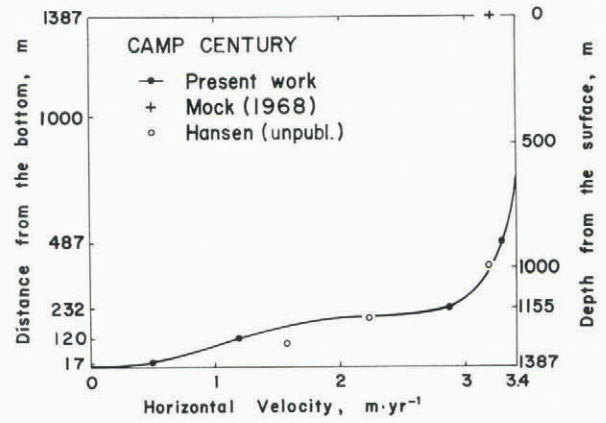
Dye 3

0 - 500	1	1	1
500 - 1 300	2	1	2
1 300 - 1 786	3	1	3
1 786 - 1 937	4	3	12
1 937 - 2 037	4	1	4

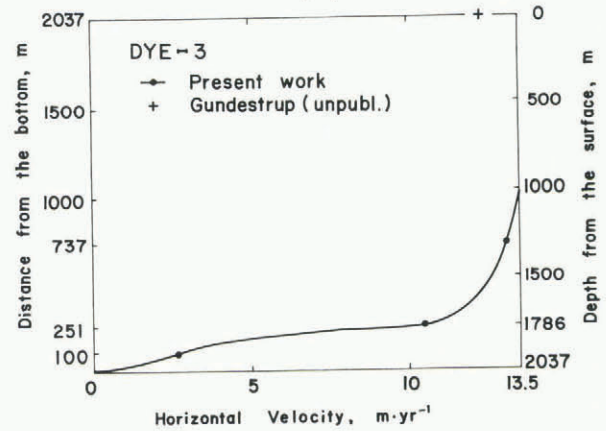
\*Total factor = fabric factor x impurity factor

depth intervals were calculated using an empirical flow law obtained by Barnes and others (1971), and the enhancement factor mentioned above (assuming laminar flow). At Dye 3, the surface slope is  $3.3 \times 10^{-3}$  rad (Overgaard and Gundestrup 1982) and the temperature profile in the bore hole has been measured by Gundestrup and Johnsen (1982). Fabric studies on the Dye 3 ice core were made by Herron [S L] and others (1982). The surface velocities calculated for Camp Century ( $3.4 \text{ m a}^{-1}$ ) and Dye 3 ( $13.5 \text{ m a}^{-1}$ ) agree quite well with the value of  $3.3 \text{ m a}^{-1}$  measured at Camp Century and that of  $12.3 \text{ m a}^{-1}$  at Dye 3 (N Gundestrup private communication). The velocity profiles obtained are shown in Figure 4. The results obtained from borehole tilting measurements at Camp Century (B L Hansen private communication) are shown in Figure 4(a) for the bottom 300 m. Hansen's results show a higher strain-rate at shallow depths than our calculation, and a value of  $5.5 \text{ m a}^{-1}$  for surface velocity.

The horizontal velocity pattern calculated for Camp Century (Fig.4(a)) is quite similar to that calculated by Weertman (1968) except for two features: (1) the flow deformation of the ice sheet is highly concentrated within the Wisconsin depth interval, and



(a)



(b)

Fig.4. Smoothed horizontal velocity profiles calculated for Camp Century and Dye 3. Strain-rate calculations were made on each slab section at 10 to 100 m depth intervals (a greater spacing was used at shallow depths). Solid circles are calculated points at the depths for which the enhancement factor changes are deduced. Open circles shown in (a) were obtained from bore hole tilting measurements by B L Hansen (private communication).

(2) the shear strain-rate decreases with depth for the lowest 125 m. These same features are also shown in the calculated velocity pattern for Dye 3 (Fig. 4(b)).

4(c). Depth-age profile

When calculating a depth-age relationship for the Camp Century core using the velocity profile obtained in this work, and assuming a two-dimensional steady-state flow as used by Dansgaard and Johnsen (1969), we obtain comparable results to time scale 1. Our analysis shows that time scale 2 (Dansgaard and others 1982) is completely different from time scale 1 (calculated with ice-flow modeling of Dansgaard and Johnsen (1969)) for the bottom 250 m at Camp Century. The apparent discrepancy may result from variations in the horizontal velocity from those of the present day which occurred during the Wisconsin. The differences may be due to temperature, ice thickness, surface slope or enhancement factor differences, and accumulation rate was also probably different in the past. On the other hand, flow behavior can be estimated from time scale 2 itself. The time scale can be converted into an annual-layer thickness profile corresponding to the vertical velocity profile under a steady-state assumption. When a two-dimensional flow model is applied, the horizontal velocity pattern can be calculated from incompressibility conditions. This is an inverse procedure of the one used by Dansgaard and

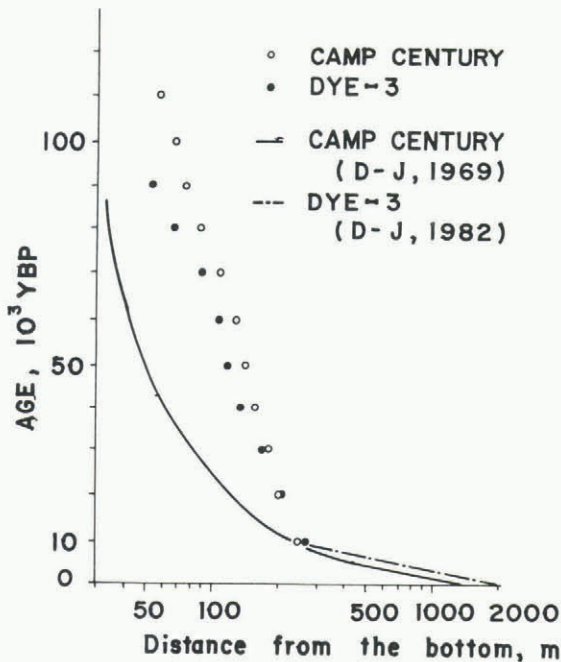


Fig.5. Depth-age profiles for Camp Century and Dye 3. Open and solid circles (time scale 2) are obtained from  $\delta^{18}\text{O}$  measurements. Solid line for Camp Century (time scale 1) was obtained by Dansgaard and Johnsen (1969). Broken line for Dye 3 (time scale 1) was obtained with Dansgaard and Johnsen's model by Dansgaard and Reeh (1982).

Johnsen (1969) in which time scale 1 was calculated from the horizontal velocity pattern. It should be kept in mind, however, that additional hypotheses require additional assumptions. For these reasons, depth-age profiles for the Camp Century and Dye 3 ice cores have been plotted with log/lin axes on Figure 5. The depth-age profile so plotted gives a straight line when the vertical strain-rate is constant with depth. Time scale 2 for both the Camp Century and Dye 3 ice cores are apparently linear for the bottom 250 m. Such a constant vertical strain-rate can be expected under a two-dimensional steady-state condition only when basal sliding is taking place. As discussed earlier, liquid lenses and veins were observed in type 1 (dark) ice in conjunction with debris particles which were incorporated from the base (Herron [S L] and Langway 1979). This indicates it is not only the pressure-melting mechanism which can cause basal melting. Another possibility arises when three-dimensional flow occurs, as would be expected from the large amplitude of the basal irregularities compared with the ice thickness observed along the Dye 3 flow line (Overgaard and Gundestrup 1982). A constant vertical strain-rate might be attained if the transversal strain-rate compensates the longitudinal strain-rate as required by an incompressibility condition under a steady-state assumption.

#### ACKNOWLEDGMENTS

Earlier discussions of theory with Dr J F Nye were instructive, and later discussions with Dr C U Hammer were very helpful. We thank Dr B L Hansen, Dr N Gundestrup, Dr A Higashi and Mr N Azuma for making available their unpublished data. This work was supported by the US National Science Foundation, Division of Polar Programs.

#### REFERENCES

Azuma N Unpublished Mechanical properties and textural change of Antarctic deep ice cores. (MS thesis, Hokkaido University, 1982)

- Barnes P, Tabor D, Walker J C F 1971 The friction and creep of polycrystalline ice. *Proceedings of the Royal Society of London Ser A* 324(1557): 127-155
- Dansgaard W, Johnsen S J 1969 A flow model and a time scale for the ice core from Camp Century, Greenland. *Journal of Glaciology* 8(53): 215-223
- Dansgaard W, Reeh N 1982 Climatic interpretation of GISP ice core data. *Eos. Transactions, American Geophysical Union* 63(18): 298
- Dansgaard W, Johnsen S J, Møller J, Langway C C Jr 1969 One thousand centuries of climatic record from Camp Century on the Greenland ice sheet. *Science* 166(3903): 377-381
- Dansgaard W and 6 others 1982 A new Greenland deep ice core. *Science* 218(4579): 1273-1277
- Duval P, Le Gac H 1982 Mechanical behaviour of Antarctic ice. *Annals of Glaciology* 3: 92-95
- Glen J W 1955 The creep of polycrystalline ice. *Proceedings of the Royal Society of London Ser A* 228(1175): 519-538
- Gundestrup N, Johnsen S J 1982 A battery powered, instrumented deep ice core drill for liquid filled holes. *Eos. Transactions, American Geophysical Union* 63(18): 297
- Hammer C U 1977[a] Dating of Greenland ice cores by microparticle concentration analyses. *International Association of Hydrological Sciences Publication* 118 (General Assembly of Grenoble 1975 - Isotopes and Impurities in Snow and Ice): 297-301
- Hammer C U 1977[b] Dust studies on Greenland ice cores. *International Association of Hydrological Sciences Publication* 118 (General Assembly of Grenoble 1975 - Isotopes and Impurities in Snow and Ice): 365-370
- Hammer C U, Clausen H B, Dansgaard W, Gundestrup N, Johnsen S J, Reeh N 1978 Dating of Greenland ice cores by flow models, isotopes, volcanic debris, and continental dust. *Journal of Glaciology* 20(82): 3-26
- Hansen B L, Langway C C Jr 1966 Deep core drilling in ice and core analysis at Camp Century, Greenland 1961-1966. *Antarctic Journal of the United States* 1(5): 207-208
- Hays J D, Imbrie J, Shackleton N J 1976 Variations in the Earth's orbit: pacemaker of the ice ages. *Science* 194(4270): 1121-1132
- Herron M M, Langway C C Jr 1982 Chloride, nitrate and sulfate in the Dye 3 and Camp Century, Greenland ice cores. *Eos. Transactions, American Geophysical Union* 63(18): 298
- Herron S L, Langway C C Jr 1979 The debris-laden ice at the bottom of the Greenland ice sheet. *Journal of Glaciology* 23(89): 193-207
- Herron S L, Langway C C Jr 1982 A comparison of ice fabrics and textures at Camp Century, Greenland and Byrd station, Antarctica. *Annals of Glaciology* 3: 118-124
- Herron S L, Langway C C Jr, Brugger K A 1982 Ultrasonic velocities and crystalline anisotropy in the ice core from Dye 3, Greenland. *Eos. Transactions, American Geophysical Union* 63(18): 297
- Higuchi K 1958 The etching of ice crystals. *Acta Metallurgica* 6(10): 636-642
- Hooke R L, Dahlin B B, Kauper M T 1972 Creep of ice containing dispersed fine sand. *Journal of Glaciology* 11(63): 327-336
- Jones S J, Glen J W 1969 The effect of dissolved impurities on the mechanical properties of ice crystals. *Philosophical Magazine* 19(157): 13-24
- Langway C C Jr 1958 Bubble pressures in Greenland glacier ice. *International Association of Scientific Hydrology Publication* 47 (Symposium of Chamonix - Physics of the Motion of Ice): 336-349
- Lile R C 1978 The effect of anisotropy on the creep of polycrystalline ice. *Journal of Glaciology* 21(85): 475-483
- Matsuda M 1979 Determination of  $\alpha$ -axis orientations of polycrystalline ice. *Journal of Glaciology* 22(86): 165-169

- Miller S L 1969 Clathrate hydrates of air in Antarctic ice. *Science* 165(3892): 489-490
- Mock S J 1968 Snow accumulation studies on the Thule peninsula, Greenland. *CRREL Research Report* 238
- Muguruma J 1969 Effects of surface condition on the mechanical properties of ice crystals. *British Journal of Applied Physics* 2(11): 1517-1525
- Nakamura T, Jones S J 1973 Mechanical properties of impure ice crystals. In Whalley E, Jones S J, Gold L W (eds) *Physics and chemistry of ice. Papers presented at the Symposium on the physics and chemistry of ice held in Ottawa, Canada, 14-18 August, 1972*. Ottawa, Royal Society of Canada: 365-369
- Nye J F 1957 The distribution of stress and velocity in glaciers and ice-sheets. *Proceedings of the Royal Society of London Ser A* 239(1216): 113-133
- Oguro M 1975 Growth of ice single crystals from dilute aqueous solutions by the modified Bridgman method - distribution of impurities and structure of dislocations. *Hokkaido University. Faculty of Engineering. Bulletin* 74: 83-94
- Overgaard S, Gundestrup N 1982 Influence of upstream topography on the Dye 3 core. *Eos. Transactions, American Geophysical Union* 63(18): 297-298
- Petit J-R, Briat M, Royer A 1981 Ice-age aerosol content from East Antarctic ice core samples and past wind strength. *Nature* 293(5831): 391-394
- Russell-Head D S, Budd W F 1979 Ice-sheet flow properties derived from bore-hole shear measurements combined with ice-core studies. *Journal of Glaciology* 24(90): 117-130
- Shoji H 1978 Stress-strain tests of ice core drilled at Mizuho station, East Antarctica. *National Institute of Polar Research. Memoirs. Special Issue* 10: 95-101
- Shoji H Unpublished Solid state physics study of Antarctic deep core ice. (Ph D thesis, Hokkaido University, 1978)
- Shoji H, Higashi A 1978 X-ray diffraction topographic studies of Antarctic deep core ice. *Japanese Journal of Applied Physics* 17(6): 993-1001
- Shoji H, Langway C C Jr 1982[a] Air hydrate inclusions in fresh ice core. *Nature* 298(5874): 548-550
- Shoji H, Langway C C Jr 1982[b] Mechanical property of fresh ice core from Dye 3, Greenland. *Eos. Transactions, American Geophysical Union* 63(18): 297
- Shoji H, Langway C C Jr 1983 Volume relaxation of air inclusions in fresh ice core. *Journal of Physical Chemistry* 87(21): 4111-4114
- Weertman J 1968 Comparison between measured and theoretical temperature profiles of the Camp Century, Greenland, borehole. *Journal of Geophysical Research* 73(8): 2691-2700